Eur. Phys. J. D **17**, 43–48 (2001)

THE EUROPEAN PHYSICAL JOURNAL D

EDP Sciences

Laser-induced fluorescence measurements of $a^3\Pi$ metastable carbon monoxide in a high enthalpy flow

P. Boubert[a] and P. Vervisch[b]

CORIA[c], Université et INSA de Rouen, 76821 Mont-Saint-Aignan Cedex, France

Received 9 April 2001 and Received in final form 13 June 2001

Abstract. Excitation of carbon monoxide molecules has been carried out in a cold cell and in a low-pressure plasma jet using an ArF narrow-band excimer laser. The different excitation models are discussed and the relevance of atomic carbon absorption into the laser cavities is pointed out. Excitation spectra of Cameron bands have been obtained in a room-temperature cell and compared with calculated spectra. A value of the constant σ related to the interaction strength between $a^3\Pi(v=2)$ state and its neighbouring singlet states is derived: $0 \leq \sigma \leq 0.05$. The fluorescence spectrum following broad band excitation of CO has been observed both in UV and visible. Similar experiments carried out in a high enthalpy flow have allowed to point out the presence of $a^3\Pi$ metastable carbon monoxide. A method for relative measurements of this species concentration is proposed.

PACS. 52.70.Kz Optical (ultraviolet, visible, infrared) measurements – 39.30.+w Spectroscopic techniques – 33.80.-b Photon interactions with molecules

1 Introduction

Carbon monoxide is an important species in combustion studies and in the area of atmospheric chemistry and pollution. Its role is also predominant in problems involving the entry of a spacecraft in the Martian atmosphere. The latter is mainly made up of carbon dioxide [1] which is highly dissociated in the shock layer in front of the thermal protect system (TPS) of the spacecraft. Through its fourth positive system ($A^1\Pi - X^1\Sigma^+$), CO is known to be one of the most radiative species.

A second source of radiation is, in spite of their low transition probabilities [2], the Cameron bands whose upper state is the metastable one, $a^3\Pi$. This triplet electronic state intervenes in some physico-chemical processes such as excitation of NO for example; it is also the final state in the de-excitation of CO($A^1\Pi$) by electrons or by heavy species. So, CO($a^3\Pi$) seems to be a significant energy carrier in the Martian upper atmosphere in conditions encountered during a spacecraft entry. It would play the same role as N_2 metastable state $A^3\Sigma^+$ in the atmosphere of the Earth.

Then, the measurement of CO (on its metastable and ground states) is a key parameter in high enthalpy facilities using CO_2 as test gas.

As it will be mentioned in the second section of this paper, the metastable state of CO is the first stage of the photodissociation of CO by an ArF excimer laser. The following fluorescence of carbon atoms should allow the measurements of carbon monoxide density in a CO_2–N_2 low pressure plasma jet. In the first part of this paper, CO excitation is studied in a room-temperature cell in order to point out the excitation processes and spectrum characteristics. This preliminary study should help to understand the mechanisms of CO laser excitation in high enthalpy media. Results and observations about experiments carried out in a CO_2–N_2 low pressure plasma jet are exposed in the second main part of the paper.

2 Experimental

The experiments have been carried out both in a low-pressure test cell and in a low-density plasma wind tunnel. The test cell is a very simple stainless steel cylindrical box (1 000 cm^3) closed with three fused silica windows and designed for cold gas (less than few hundred Kelvin) measurements. In this study, the cell is filled with pure CO under a pressure of 50 hPa. Two symmetric windows are used for laser access and a third lateral one is used for fluorescence detection by receiving a photomultiplier.

Some measurements have also been performed in a larger test chamber, first in cold CO under pressure up to 200 hPa, and second in a low-pressure CO_2–N_2 plasma jet. In this case, the pressure in the test chamber is 1 hPa;

[a] *Present address:* IUSTI, Université de Provence, 13453 Marseille Cedex 13, France.
e-mail: boubert@iusti.univ-mrs.fr
[b] e-mail: pierre.vervish@coria.fr
[c] UMR 6614 du CNRS

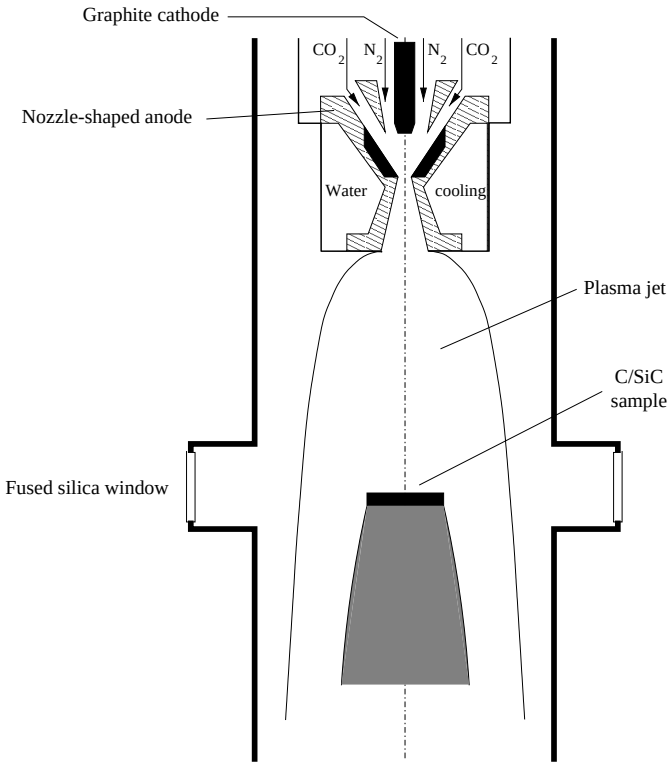

Fig. 1. The plasma generator with the C/SiC tile into the plasma flow.

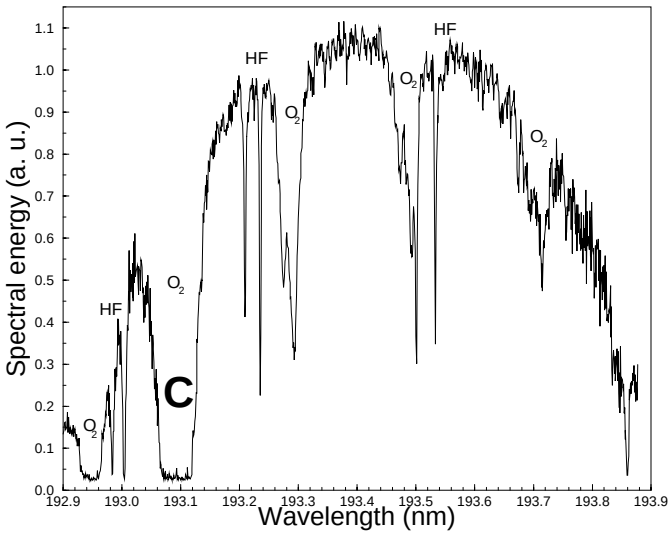

Fig. 2. Spectral energy of the ArF tunable excimer laser with absorption bands of O_2, HF and C.

this pressure is obtained thanks to the coupling of a primary pump and a roots pump. A dc 9 kW arc is established between a carbon cathode and a carbon crown crimped in a nozzle-shaped copper anode. The use of high purity graphite as electrode material has allowed the avoidance of pollution of the flow by metallic species. Such a precaution is necessary when oxidizing atoms and molecules, as atomic oxygen and carbon monoxide are present in the arc chamber. Both electrodes are water-cooled. Carbon dioxide and nitrogen mass flow rate are equal to 0.18 g/s. Nitrogen is injected along the cathode to cool it and to protect it from the action of oxidizing species, while injection of carbon dioxide is made along the anode. During the first minutes of working, there is an erosion of the carbon electrodes until the establishment of a steady state. The anode is conical both upstream (30°) and downstream (13°) from the 5 mm throat. Then the pressure in the arc chamber is about 200 hPa and the jet is supersonic at the outlet of the plasma source with a shock located at about 40 mm downstream from the nozzle exit. Measurements are carried out 100 mm downstream in a low-gradient region where the plasma is subsonic and where both temperatures and densities are homogeneous according to LIF and emission spectroscopy measurements carried out on several species. The free stream as well as the boundary layer over a C/SiC tile are studied. A scheme of the wind tunnel is shown in Figure 1.

Excitation of the different media is achieved thanks to an ArF tunable excimer laser (Lambda Physik LPX150/50T). This source is tunable over a range of 1 nm centered around 193.4 nm with an energy close to 180 mJ. Within this study, the energy of each pulse is limited to 100 mJ. An amplifying cavity is pumped by the radiation created and spectrally refined in an oscillator cavity. In narrow-band mode the linewidth is 0.3 cm^{-1}. The spectral energy of the ArF laser at the test point is shown in Figure 2.

For experiments in the low-pressure cell, as the medium is made up of pure CO, a fast photomultiplier is directly set in front of the lateral window in order to collect a maximal number of photons. For experiments in the plasma, because of the fluorescence of other species excited by the ArF laser (especially NO), the studied fluorescence is monitored through a Czerny-Turner spectrometer ($f = 588$ mm) used with a 3 600 gr/mm grating whose dimensions are 110×80 mm. The optical system is set to obtain a 1 mm×1 mm resolution in the plasma. In each case Philips XP2020/Q fast photomultipliers (bialkaline photocathode and 1.5 ns anode rise time) are used. Both experiments, in the low-pressure cell and in the plasma, could be carried out simultaneously tanks to dielectric mirrors whose reflectivity is 95%. The general experimental set-up is depicted in Figure 3.

3 Excitation models

ArF laser radiation is known to be able to excite carbon monoxide up to dissociation and ionisation. Hill *et al.* [3] studied competition between both phenomena and found a complete domination of multiphoton dissociation up to 30 GW/cm^2. The power density of the ArF laser is about 5 GW/cm^2 so multiphoton ionisation will be neglected in the following. The first step of multiphoton dissociation of CO is the absorption of an ArF photon from the ground state $X^1\Sigma^+(v = 0)$ to the metastable state $a^3\Pi(v = 2)$ [4].

The fluorescence observed from excitation of CO with ArF radiation is due to the de-excitation of produced

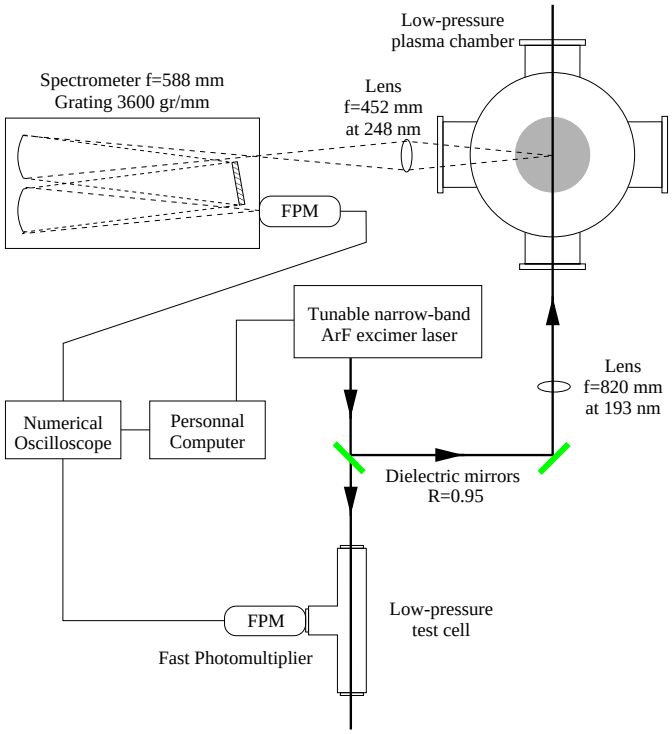

Fig. 3. General experimental set-up for the plasma wind tunnel and the test cell.

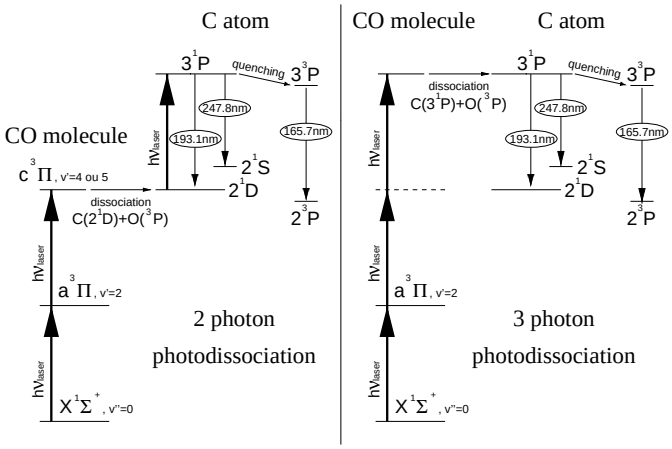

Fig. 4. Models for CO photodissociation and atomic carbon fluorescence.

excited carbon atoms, and is detected at three wavelengths: 165.7, 193.1 and 247.8 nm. Two models are available to explain the production of 3^1P carbon atoms from the metastable state. The first one proposes the excitation of the CO molecule from the metastable state to a $c^3\Pi(v = 4, 5)$ Rydberg state [3]. This state is predissociated by a $^3\Pi$ valence state which leads to the formation of C(2^1D). This resulting atom is then excited thanks to a third photon of the same laser pulse at the wavelength 193.09 nm to produce C(3^1P) atom. In spite of the three photons involved, this process induces a quadratic variation of fluorescence with the laser energy; indeed the last step, the absorption of the third photon by a carbon atom is fully saturated. The second process, according to Meijer *et al.* [4], assumes the absorption of two photons from the metastable state to the dissociative continuum to produce directly C(3^1P) atoms. In this case the dependence of fluorescence intensity with the laser energy is cubic since there is no saturated step. Such a cubic variation has been measured during the experiments in cold gas reported here.

Both models are summarized in Figure 4. The laser used in the present study is unable to produce any photon at 193.09 nm because of an intracavity absorption by atomic carbon. So, the fluorescence observed can not come from the de-excitation of an atom excited through the first process since the laser is unable to excite atomic carbon from its 2^1D state to its 3^1P state. Within this study, only the three-photon dissociation of CO is able to induce the fluorescence of atomic carbon. In fact, CO is certainly dissociated through both processes with a higher probability for the two-photon one, but excited atomic carbon can only be produced by the three-photon process. In our experimental configuration the fluorescence of carbon atoms is detected at 247.8 nm only. Indeed on the one hand the detection of the 165.7 nm fluorescence imply an optical axis under vacuum to avoid absorption by the Schumann-Runge bands of molecular oxygen of air; on the other hand the detection at 193.1 nm is disturbed by spontaneous emission of atomic carbon produced in the plasma jet and by the fluorescence of ϵ bands of NO also produced in the CO_2–N_2 plasma. Whatever the excitation process, resulting oxygen atom are produced on the fundamental state and are not involved in the fluorescence process. Molecular oxygen contribution has been shown to be negligible [10].

4 Cold measurements and spectral simulation

Experimental excitation spectra of CO have been obtained in a cold cell filled with 50 hPa of CO by scanning the tunable range of the ArF laser. One of these experimental spectra is shown at the top of Figure 5. Whatever the photodissociation process, the first step is the absorption of an ArF photon along the forbidden transition:

$$X^1\Sigma^+(v'' = 0) \rightarrow a^3\Pi(v' = 2).$$

Because of the low band strength of this transition in regards to those of the next transitions, this step is the limitative one. So, the lines observed on the experimental spectrum correspond to those of the Cameron band $a(v' = 2)$–$X(v'' = 0)$.

The quite Gaussian shape of the laser spectrum is visible in Figure 5 in the envelope of the line spectrum as well as in the broad band background. For each excitation wavelength, the measurement corresponds to the mean value of 32 laser shots. With three-photon excitation, fluorescence intensity is proportional to E^3_{laser} where E_{laser} is the energy of the laser pulse. Shot-to-shot fluctuations of this laser energy have been shown to be less than 5%

during the acquisition time of the experimental excitation spectrum. This nearly constant energy allows us to assume that $\langle E_{\rm laser}^3 \rangle \approx \langle E_{\rm laser} \rangle^3$. A simulation of the experimental excitation spectrum may then be obtained knowing the laser spectral energy (Fig. 2), the temperature of the experiment, the rovibronic energy levels of $X^1\Sigma^+$ and $a^3\Pi$ states [5,6], and the line strengths of Cameron transitions [7]. The expressions for the Hönl-London factors for a ${}^3\Pi \leftarrow {}^1\Sigma$ transition are given below:

$$S_{\rm P_1}(J+1) = \frac{J(J+1)^2}{4C_1(J)} \left\{\sigma u_1^+(J) - 2(J-1)\right\}^2$$

$$S_{\rm Q_1}(J) = \frac{(J-1)^2(J+1)^2(2J+1)}{C_1(J)}$$

$$S_{\rm R_1}(J-1) = \frac{J}{2C_2(J)} \left\{(Y-2) + 2\sigma(J+1)\right\}^2$$

$$S_{\rm P_2}(J+1) = \frac{J}{2C_2(J)} \left\{(Y-2) + 2\sigma(J+1)\right\}^2$$

$$S_{\rm Q_2}(J) = \frac{2J+1}{2C_2(J)}(Y-2)^2$$

$$S_{\rm R_2}(J-1) = \frac{J+1}{2C_2(J)} \left\{(Y-2) - 2\sigma J\right\}^2$$

$$S_{\rm P_3}(J+1) = \frac{J}{4C_3(J)} \left\{(J+1)\sigma u_3^-(J) + 2J(J+2)\right\}^2$$

$$S_{\rm Q_3}(J) = \frac{J^2(J+2)^2(2J+1)}{C_3(J)}$$

$$S_{\rm R_3}(J-1) = \frac{J^2(J+1)}{4C_3(J)} \left\{\sigma u_3^-(J) - 2(J+2)\right\}^2$$

where

$$u_1^+(J) = \sqrt{Y(Y-4) + 4J^2} + Y - 2$$
$$u_3^+(J) = \sqrt{Y(Y-4) + 4(J+1)^2} - Y + 2$$
$$C_1(J) = Y(Y-4)J(J+1) + 2(2J+1)(J-1)J(J+1)$$
$$C_2(J) = Y(Y-4) + 4J(J+1)$$
$$C_3(J) = Y(Y-4)J(J+1) + 2(2J+1)J(J+1)(J+2).$$

$Y = A/B$ is a constant which quantifies the coupling of rotation and electronic motions. A is the spin-orbit interaction constant and B the rotational constant related to the moment of inertia. The values of A and B for the vibrational quantum number $v = 2$ are calculated from [5]. Each Hönl-London factor is normalized by $2J+1$. Simulations of the excitation spectrum have been performed both with calculated and experimental wavenumbers without any significative difference.

Cameron transitions are only allowed thanks to the coupling of $a^3\Pi$ and $A^1\Pi$ states. For the low rotational quantum numbers, the coupling is especially strong for the $\Omega = 1$ component of the metastable state [2,8]. The mixing increases with J, the intensity of transitions involving $\Omega \neq 1$ levels increases as well. This phenomenon is taken into account in the calculation of the line intensities by a parameter called σ. This constant is related to the interaction strength between the ${}^3\Pi$ state and its neighbouring singlet states [7] which is independent in regards to the rotational quantum number J [9]. According to Schlapp and Kovács, σ corresponds to the ratio between the $\mu({}^1\Sigma^+ - {}^1\Sigma^+)$ and $\mu({}^1\Pi - {}^1\Sigma^+)$ contributions to the $a-X$ transition moment borrowed from parallel and perpendicular allowed transitions. To our knowledge, no quantitative value is known for this parameter. In their study about the 0–0 Cameron band, White *et al.* estimated it to about 0.15 for $v = 0$ by comparison with their experimental spectra. So, this value has been used as a default one in the simulation of the excitation spectrum but it was possible to obtain better results by taking σ as a free parameter in the calculations. Within the whole excitation spectrum, an estimation may be obtained by comparison of Q-branch relative intensity, which are independent of σ, with R- and P-branch relative intensities, which depend on σ value. An expanded view is shown in Figure 6 for the experimental spectrum and some calculated spectra corresponding to three values of σ. The best agreement after a minimization of the square of the difference between experimental and calculated peak intensities is obtained for a value close to 0: $\sigma = 0.02$. Considering the uncertainty of the method, σ can be told included in the range (0, 0.05). The best simulation is shown at the bottom of Figure 5.

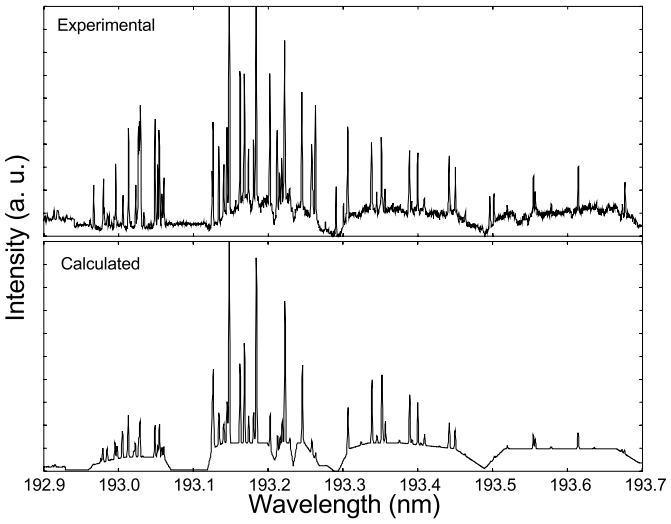

Fig. 5. Experimental (top) and calculated (bottom) excitation spectra of CO at 300 K.

Fluorescence spectra following a broad band excitation of cold CO has also been recorded. In fact a green fluorescence is clearly visible to the naked eye along the laser path in the test chamber or in the test cell for pressure down to 15 hPa. This radiation obviously comes from the de-excitation of the $d^3\Pi$ of C_2 along the famous Swan bands. Classically, C_2 may be formed through the three body reaction:

$$\mathrm{C} + \mathrm{C} + \mathrm{M} \rightarrow \mathrm{C_2} + \mathrm{M}$$

where M is a collision partner.

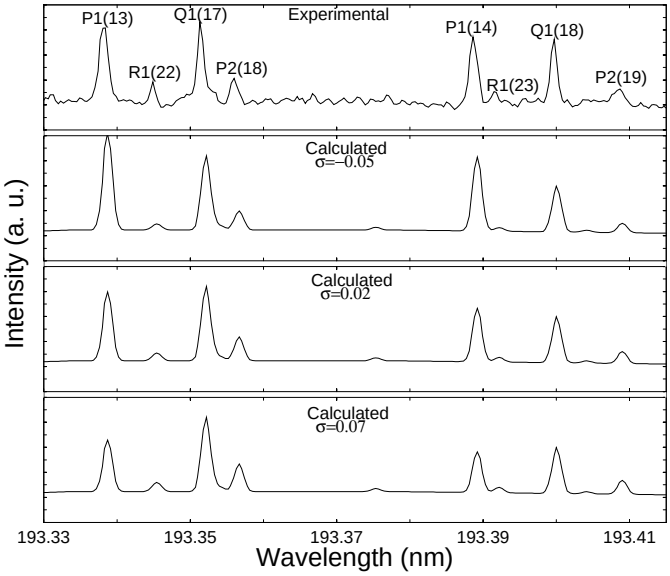

Fig. 6. Comparison between the intensities of a few P-, Q- and R-lines for three value of σ.

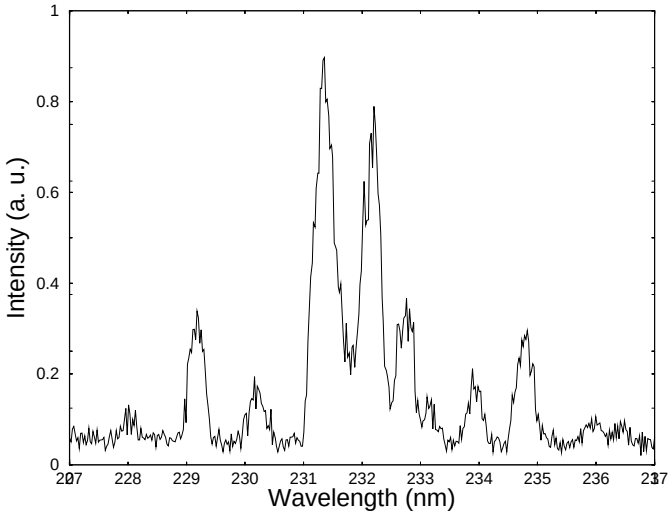

Fig. 7. Fluorescence spectrum near 230 nm following the broad band excitation of cold CO.

Nevertheless, considering the low pressure of the experiment, an other process seems more probable:

$$\mathrm{CO}(a^3\Pi) + \mathrm{C} \rightarrow \mathrm{C_2} + \mathrm{O}$$

since the reactants are both produced during the excitation of CO.

The fluorescence has also been observed in the UV range of wavelengths. A part of the spectrum near 230 nm is the subject of Figure 7; it shows the overlap of fluorescence along the 0–0 band of the Mulliken system ($D^1\Sigma_u^+ \rightarrow X^1\Sigma_g^+$) of C_2 and several bands of the first negative system ($B^2\Sigma^+ \rightarrow X^2\Sigma^+$) of CO^+. The part of the spectrum between 300 and 370 nm is also very rich including the third positive system of CO, the tail comet system of CO^+ and the Fox-Herzberg and Deslandres-d'Azambuja systems of C_2.

However, these fluorescences remain much lower than atomic carbon fluorescence and can not disturb the measurements made without UV-filter or spectrometer.

5 Measurements in a CO_2–N_2 plasma jet

The main purpose of this study was to measure CO evolution and densities in the boundary layer of a thermal protection tile (C/SiC) in a CO_2–N_2 plasma jet (Fig. 1). As said before, the plasma is generated through a dc arc from an equal mass fraction mixture of CO_2 and N_2. The material used is a tile of C/SiC made by Société Européenne de Propulsion (SEP/SNECMA) in Bordeaux (France). It consists of a 30 mm disc positioned perpendicularly to the plasma axis to maximise the flux on the surface.

In this facility, the chamber pressure is 1 hPa, *i.e.* two orders of magnitude less than in cold experiments. Nevertheless, first measurements gave a fluorescence signal 50 times higher than in cold experiments carried out with the same optical set-up. The kinetic temperature of the plasma has been estimated through the rotational temperature of nitrogen monoxide ground state (2 500 K) also measured by laser-induced fluorescence [10]. So, there is an increase of the population of rotational levels absorbing the laser radiation ($7 \leq J \leq 23$) due to the higher temperature in the plasma. However, this increase is not sufficient to explain the so high fluorescence signal collected from the plasma. As the laser produces no photon at 193.09 nm, it is unable to excite atomic carbon present in the plasma jet (whose density is assumed to be low [11]). Moreover a quadratic variation of the fluorescence intensity with the laser energy has been observed (Fig. 8) instead of the cubic variation which matched in cold experiments.

In the three photon dissociation of CO, the hardest step is the first one because of the forbidden character of the Cameron transitions. If this first excitation is already performed during the plasma creation, metastable CO is present in the medium and just two photons are required to dissociate the molecule and induce the fluorescence of carbon atoms. This process leads to a higher efficiency of excitation and justify the quadratic variation of the fluorescence intensity with the laser energy.

This hypothesis is confirmed by the narrow-band excitation. Indeed, since the absorption

$$X^1\Sigma^+(v''=0) \rightarrow a^3\Pi(v'=2)$$

is no more the main source of excited atomic carbon, the excitation spectrum should not represent this transition but rather the absorption from the metastable state to the dissociative continuum. Experimentally, the excitation spectrum recorded in the plasma was effectively no more a line spectrum but a continuous one.

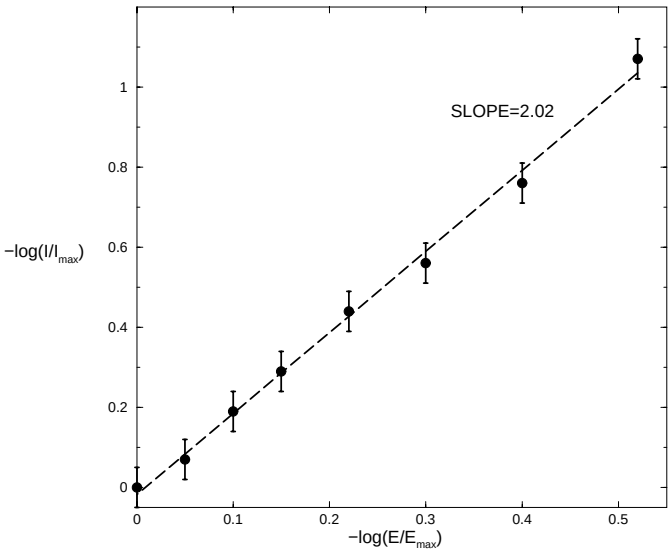

Fig. 8. Quadratic variation of the fluorescence I with the laser energy E in the plasma, $30 \leq E \leq 100$ mJ.

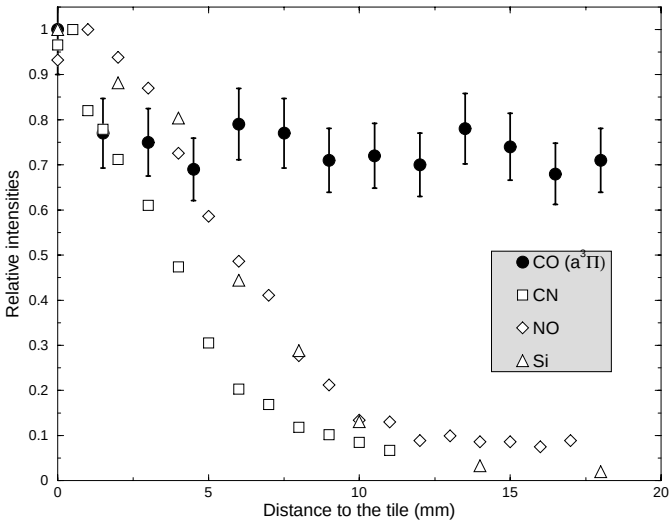

Fig. 9. Evolution of CO($a^3\Pi$), CN, NO and Si densities in the boundary layer over a C/SiC tile.

Considering the relative probabilities of the three photon photodissociation from the ground state on the one hand, and of the two photon photodissociation from the metastable state on the other hand, the detected fluorescence of atomic carbon is definitively representative of the density of the metastable state of CO.

Considering the pressure of the experiment, a complete dissociation of CO_2 and a high value for electronic excitation, an estimation of the density of metastable CO in the plasma jet shows that it is less than 2×10^{12} cm^{-3}. This highest value means that excitation by ArF laser is a very sensitive detection technique of metastable CO. Considering the signal levels obtained in the plasma jet, with a signal/noise ratio close to 200, excitation of metastable CO is sensitive enough to measure absolute density down to 10^{10} cm^{-3}. A calibration of the measurement could be made by absorption in a long homogeneous discharge to obtain absolute densities.

In the case of the boundary layer studied here, no significant variation of metastable CO density has been noticed unlike other species as CN, NO and Si [11]. The evolution of the four species in the boundary layer are shown in Figure 9. Then, no recombination of metastable CO seems to occur on the C/SiC tile.

6 Conclusions

A study on the excitation of carbon monoxide by an ArF laser has been carried out, first in a test cell with cold gas (300 K), then in a CO_2–N_2 low-pressure arc-jet. In the first case, narrow-band excitation allowed to point out an absorption of the laser radiation by atomic carbon inside its own cavities, and then to favour a three photon dissociation model. Moreover, a comparison between the experimental and synthetic excitation spectra gave an estimation of the coupling parameter σ for $a^3\Pi(v = 2)$.

An unexpected very strong fluorescence signal observed in the plasma and its quadratic dependence in regard to the laser energy has led us to propose the hypothesis of the presence of metastable CO in the plasma before laser excitation. This result is important for people wishing to measure CO total density evolutions in this kind of media. Nevertheless, measurements of metastable CO density evolutions, which used to be difficult, could be performed by this way. The density of the ground state of CO would better be measured by two-photon LIF at 230 nm. An ArF laser coupled with a hydrogen-filled Raman shifter are able to provide those photons.

References

1. A. Seiff, D. Kirk, J. Geophys. Res. **82**, 4364 (1977).
2. T. Sykora, C. Vidal, J. Chem. Phys. **110**, 6319 (1999).
3. W.T. Hill, B.P. Turner, H. Lefebvre-Brion, S. Yang, J. Zhu, J. Chem. Phys. **92**, 4272 (1990).
4. G. Meijer, A.M. Wodtke, H. Voges, H. Schlüter, P. Andresen, J. Chem. Phys. **89**, 1099 (1973).
5. R. Field, S. Tilford, R. Howard, J. Simmons, J. Mol. Spectr. **44**, 347 (1972).
6. R. Field, B. Wicke, J. Simmons, S. Tilford, J. Mol. Spectr. **44**, 383 (1972).
7. I. Kovács, *Rotational structure in the spectra of diatomic molecules* (Adam Hilger LTD, London, 1969).
8. T. James, J. Chem. Phys. **55**, 4118 (1971).
9. R. Schlapp, Phys. Rev. **39**, 806 (1932).
10. David Honoré, Ph.D. thesis, University of Rouen, 1995.
11. P. Boubert, P. Vervisch, J. Chem. Phys. **112**, 10482 (2000).